Electrical Power from Sea and River Water by Reverse Electrodialysis: A First Step from the Laboratory to a Real Power Plant

JOOST VEERMAN,[†,‡] MICHEL SAAKES,[†] SYBRAND J. METZ,*[,†] AND G. JAN HARMSEN[§]

Wetsus, Centre of Excellence for Sustainable Water Technology, P.O. Box 1113, 8900 CC Leeuwarden, The Netherlands, NHL Hogeschool, Department of Life Sciences and Technology, Agora 1, 8934CJ Leeuwarden, The Netherlands, and University of Groningen, Nijenborgh 4, 9747 AG Groningen, The Netherlands

Received March 24, 2010. Revised manuscript received July 15, 2010. Accepted October 7, 2010.

Electricity can be produced directly with reverse electrodialysis (RED) from the reversible mixing of two solutions of different salinity, for example, sea and river water. The literature published so far on RED was based on experiments with relatively small stacks with cell dimensions less than 10 × 10 cm^2. For the implementation of the RED technique, it is necessary to know the challenges associated with a larger system.
In the present study we show the performance of a scaled-up RED stack, equipped with 50 cells, each measuring 25 × 75 cm^2. A single cell consists of an AEM (anion exchange membrane) and a CEM (cation exchange membrane) and therefore, the total active membrane area in the stack is 18.75 m^2. This is the largest dimension of a reverse electrodialysis stack published so far. By comparing the performance of this stack with a small stack (10 × 10 cm^2, 50 cells) it was found that the key performance parameter to maximal power density is the hydrodynamic design of the stack. The power densities of the different stacks depend on the residence time of the fluids in the stack. For the large stack this was negatively affected by the increased hydrodynamic losses due to the longer flow path. It was also found that the large stack generated more power when the sea and river water were flowing in co-current operation. Co-current flow has other advantages, the local pressure differences between sea and river water compartments are low, hence preventing leakage around the internal manifolds and through pinholes in the membranes. Low pressure differences also enable the use of very thin membranes (with low electrical resistance) as well as very open spacers (with low hydrodynamic losses) in the future. Moreover, we showed that the use of segmented electrodes increase the power output by 11%.

Introduction

Salinity gradient power (SGP) is a potentially clean and sustainable form of energy; and can be generated from the reversible mixing of seawater and river water. The theoretical energy content of mixing 1 m^3 river water with a large surplus of seawater is 2.5 MJ or 1.7 MJ when mixed with 1 m^3 seawater (*1*). The global potential of SGP is estimated to be 2.6 TW (*2*) when the flow of all the rivers is taken into account. There are two membrane-based technologies which can convert this potential energy into useful electricity: reverse electrodialysis (RED) and pressure retarded osmosis (PRO). It has been shown that, in the case of river water with seawater, RED is a promising technique (*3*). This technique was first published by Pattle (*4, 5*) in 1954 and is gaining interest due to increased awareness of the use of sustainable energy sources (*6*).

Figure 1 shows the principle of RED. A number of alternately stacked cation exchange membranes (CEM) and anion exchange membranes (AEM) are separated by spacers. These spacers are open structures that are needed for structural stability of the stack and the promotion of turbulence within the compartments. The spacer filled compartments are fed alternately with seawater and river water. The cations diffuse from sea to river water compartments through the CEMs and the anions through the AEMs in the opposite direction. The ion current in the stack is converted to an electron current at the electrodes by redox reactions.

For optimal performance, a RED power plant should generate maximal power from a given river water feed at lowest investment and operational costs. Related to these economical aspects, three response parameters are important: power density, energy efficiency, and net power. A high power density (power generated per m^2 membrane) decreases investments not only in membranes but in the whole stack. High energy efficiency (the percentage of the generated energy from a given amount of feedwater compared with the theoretical limit) is favorable for the optimal use of the available water sources. Power density and energy efficiency are conflicting: for high energy efficiency large membrane

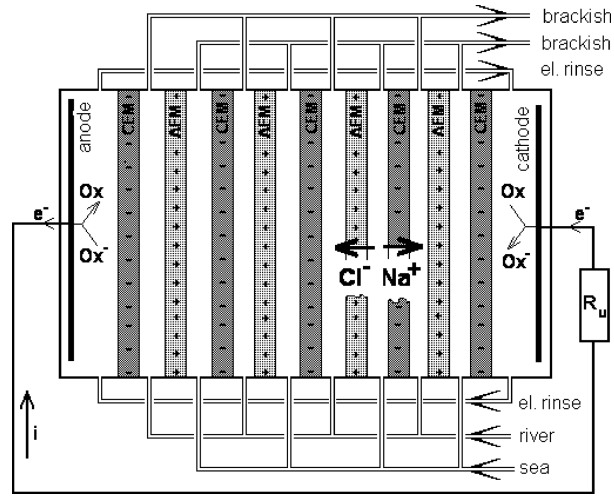

FIGURE 1. Principle of RED. Cations diffuse through CEMs from seawater to river water compartments in the direction of the cathode, anions diffuse through the AEMs in the opposite direction. The ion current in the stack is converted to an electron current at the electrodes via the reversible redox reaction Ox + e ⇔ Ox$^-$.

* Corresponding author phone: +31-58 2843 000; e-mail: sybrand.metz@wetsus.nl.
† Wetsus.
‡ NHL Hogeschool.
§ University of Groningen.

10.1021/es1009345
Published on Web 10/21/2010

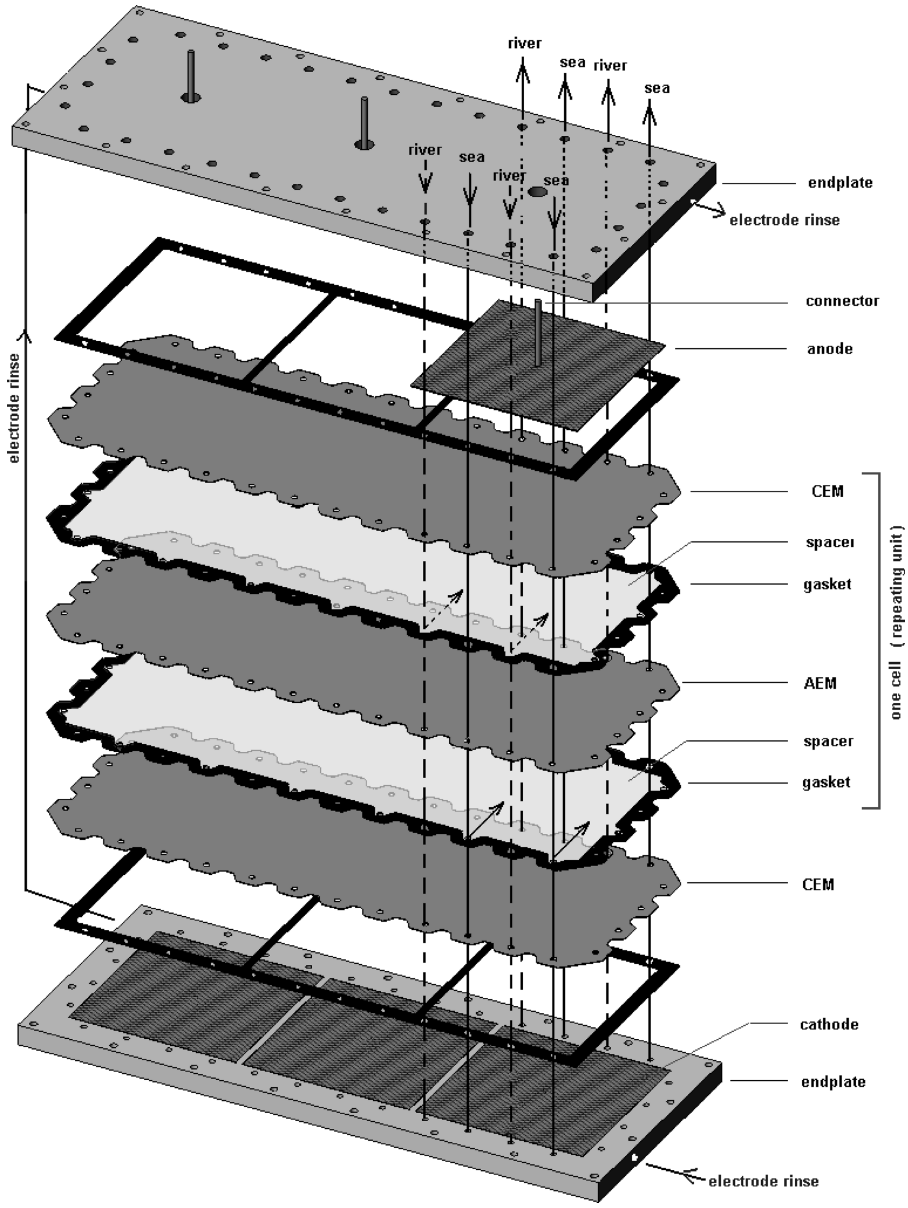

FIGURE 2. Exploded view of the large stack equipped with only one cell. The holes in the long end are used for water feed and drain in the short direction (with 25 cm flow path) as shown in the figure. Alternatively, the holes in the short side can be used for operation in the other direction (with 75 cm flow path).

areas at a low power density are necessary (*1, 7*). Hydrodynamic losses due to the pumping of water through a RED stack should be kept to a minimum. A key parameter for the hydrodynamic resistance is the length of the flow channel. If only power density and energy efficiency are maximized, the result of an optimization procedure may be a very small stack with a low power production. Therefore, the total generated power of the stack (the net power) is also an important response parameter.

Up to now all our published experimental work on RED has been done with relatively small stacks (10 × 10 cm^2) (*1, 8, 9*). In this work we compare the performance of these small laboratory stacks with an up-scaled 25 × 75 cm^2 stack. With this larger stack we will also study new aspects affecting the performance, such as: residence time, flow direction (co- or counter-current), flow velocity, segmentation of electrodes (various current densities as a function of the position in the stack).

Experimental Section

RED Stacks. Two types of stacks were investigated. The "small stack" is described in detail elsewhere (*1*) and was equipped with 50 cells of 10 × 10 cm^2 with a total membrane area of 1 m^2. In addition to this, we constructed a novel stack (called "large stack") as shown in Figure 2. In this large stack three electrode compartments—each with its own electrodes—were located on each side inside the end plates. End plates were milled from HDPE (high-density polyethylene). Not shown in this picture are the two stainless steel supporting plates, needed to prevent bending of the cell. The large stack was equipped with 25 cells of 25 × 75 cm^2 with a total membrane area of 9.4 m^2 and later on expanded to 50 cells with a total membrane area of 18.75 m.

Cells. On the outsides of the large stack, Fumasep FKD cation exchange membranes (Fumatech, Germany) were used as stable end membranes. These membranes are more resistant to chlorine, which evolved at the anode. The inner membranes were Qianqiu (Homogeneous AEM and CEM, Hangzhou Qianqiu Industry Co, China). The stacks were equipped with nylon woven spacers, thickness 200 μm (wire diameter 122 μm, porosity 67%) (Nitex 03-300/51, Sefar, The Netherlands); in some experiments with the small stack, 100 μm spacers (wire diameter 62 μm, porosity 74%) were used

(Nitex 03-190/57). Gaskets were made of silicone rubber with a thickness of 200 μm (SSF-MLTN-940, Specialty Silicone Fabricators, Paso Robles, CA).

Electrode System and Electrical Measurements. The electrode system and the measurement method were analogous to those of the small stack, which is described in detail elsewhere (*1*). However, the electrodes used in the large stack were different. Anodes were coated with Ir mixed metal oxides and the cathodes with Ru mixed metal oxides (Magneto Special Anodes, Schiedam, The Netherlands). These electrodes are optimized for one current direction. Galvanostatic measurements were carried out with an Ivium potentiostat in combination with an Ivium booster (Ivium Technologies, Eindhoven, The Netherlands) which permits measurements up to 20 A at 20 V. Two types of electrode rinse solutions were employed. In some experiments a solution of (15 g/L) NaCl (0.25 mol/L) was used. This electrolyte is electrolyzed at the electrodes and the electrolysis consumes a large part of the generated energy. However, even in the case of a net negative power production, measurements were possible through the use of a potentiostat. The effect of segmentation of the electrode was studied with the hexacyanoferrate electrode solution ($K_4Fe(CN)_6$: 0.05 mol/L, $K_3Fe(CN)_6$: 0.05 mol/L, NaCl: 0.25 mol/L). With this system electrode losses are much lower than the generated power and therefore it was possible to use three variable resistors (slide rheostats of 22 Ω, 5 A) as electrical load instead of three potentiostats and boosters. On each flow rate, IE-curves were measured; E being the voltage measured on the reference electrodes and I the applied electrical current. The generated electrical power was obtained from the maximal product of current and voltage with different loads. Power densities were achieved by dividing the power by the total active membrane area.

It should be emphasized that the applied electrode systems are only suitable for laboratory experiments. For the use in commercial RED plants, more sophisticated systems are necessary. A comparison of different electrode systems is published elsewhere (*10*).

Sea and River Water. 'Sea water' consisted of 30 g NaCl/L and "river water" of 1 g NaCl/L. A conductivity meter with a Tetracon 325 cell (WTW, Weilheim, Germany) was used. For the delivery of sea and river water and for recirculation of the electrode rinse, peristaltic pumps were used. Temperature was controlled at 298 ± 1 K for all experiments.

Flow Rate and Pressure Measurements. Flow rates were determined gravimetrically. Pressure differences were measured with a Deltabar S (Endress + Hauser, Germany) differential pressure gauge between inlet and outlets. Hydrodynamic losses were determined as the product of flow rate and pressure difference.

Results and Discussion

In this article we focus on the power production by a REDstack. Power is generated by the potential over a membrane (ΔΦ)and the transport of ions through a membrane. The relationship between the potential across a membrane and the concentration of the ions is given by eq 1:

$$\Delta\phi = \frac{\alpha RT}{zF}\ln\left(\frac{a_S}{a_R}\right) \tag{1}$$

where ΔΦ is the potential (V), α the membrane selectivity, R the gas constant (8.314 J mol^{-1} K^{-1}), T the absolute temperature (K), z the electrochemical valence (−), F the Faraday constant (96485 C mol^{-1}), a_S the activity of the concentrated salt solution (seawater) (mol L^{-1}) and a_R the activity of the diluted salt solution (river water) (mol L^{-1}).

The total potential of a RED stack is the number of membranes (n) times the potential across one membrane. Maximal power is obtained when the internal stack resistance (R_i) equals the external resistance (R_u) (*8*) given by the following relationship:

$$P_u = I^2 R_u = \left(\frac{E}{R_i + R_u}\right)^2 R_u = \frac{(n \cdot \phi)^2}{4R_i} \tag{2}$$

where P_u is the generated electrical energy. The internal stack resistance (R_i in Ωm^2) is the sum of the area specific resistances of the anion exchange membrane (R_{AEM}), the fresh water compartment, the canion exchange membrane (R_{CEM}), and salt water compartment. This can be written as follows (*14*):

$$R_i = R_{AEM} + \frac{h_R}{\varepsilon^2 \kappa_R} + R_{CEM} + \frac{h_S}{\varepsilon^2 \kappa_S} \tag{3}$$

where h is the compartment or spacer width (m), ϵ the porosity (−) of the spacer, κ the conductance of the solution (S/m); subscript R stands for the diluted compartment (river water) and subscript S for the concentrated (seawater) compartment.

In this article we distinguish between power density (P_d), the generated electrical power per m^2 membrane (AEM and CEM) and the net power density ($P_{d\text{-net}}$), the generated power density minus the hydrodynamic losses. They are determined as follows:

$$P_d = \frac{P_u}{A} \tag{4}$$

$$P_{d\text{-net}} = \frac{P_{net}}{A} \tag{5}$$

P_{net} is the generated electrical power (P_u) minus the hydrodynamic loss (P_{hydr}), A stands for the total active membrane area (AEMs and CEMs together). Some authors use the cell-pair area for A. However, we prefer the total active membrane area in order to relate to other membrane based SGP processes like pressure retarded osmosis (PRO) (*3*). The hydrodynamic losses can be described by eq 3:

$$P_{hydr} = \Phi_R \Delta P_R + \Phi_S \Delta P_S \tag{6}$$

where Φ_R and Φ_S are flow rates of river and seawater (m^3/s) and ΔP_R and ΔP_S the pressure drop (Pa) over the river and seawater compartments.

Energy efficiency is the obtained electrical energy from a given quantity of feedwater divided by the potential amount of energy; for the net energy efficiency (Y_{net}) this value is corrected for the hydrodynamic losses (*9*).

The feedwater entering a RED stack represents a certain amount of exergy X^i (*1, 11, 12*):

$$X^i = 2RT\left[\Phi_R C_R \ln\frac{C_R}{C_M} + \Phi_S C_S \ln\frac{C_S}{C_M}\right] \tag{7}$$

where X^i is the exergy flow rate if the feed (W), R is the gas constant (8.314 J·mol^{-1}K^{-1}), T temperature (K), Φ_R, and Φ_S flow rates of river and seawater (m^3/s) and C_R and C_S the salt concentrations in the river and seawater (mol/m^3). C_M is the equilibrium concentration, obtained at total mixing of river and seawater:

$$C_M = \frac{\Phi_R C_R + \Phi_S C_S}{\Phi_R + \Phi_S} \tag{8}$$

The energy efficiency Y is the part of the incoming exergy flow rate that is converted to electrical power:

$$Y = \frac{P_u}{X^i} \tag{9}$$

The net energy efficiency (Y_{net})is the amount of generated electrical power (P_u) minus the hydrodynamic loss (P_{hydr}) related to the exergy of the feedwater:

$$Y_{net} = \frac{P_u - P_{hydr}}{X^i} = \frac{P_{net}}{X^i} \tag{10}$$

Effect of the Residence Time on the Power Density. At high flow rates, it is expected that the power density is maximal because the concentration difference between the fresh and salt water on both sides of the membrane is nearly unaffected by the transport of salts through the membrane resulting a high potential difference across the membrane (eq 1). However, hydrodynamic power losses should be taken into account; these are maximal at high flow rates. Consequently, there exists an optimal flow rate for maximal net power density.

First of all only the (gross) power density was studied. Figure 3 compares data of experiments with different process parameters for two membrane types (Fumasep and Qianqiu), two stack sizes (small and large), three flow directions (cross-, co-, and counter-current), and two cell numbers (25 and 50). The main conclusion from Figure 3 is that the residence time is the key parameter governing the power density. The generated electricity in different stacks with the same spacers is largely independent of flow direction, membranes, cell dimensions and the number of cells. The small influence of the flow direction is discussed later on in this article; the independence of the membranes is most likely due to comparable membrane properties (electrical resistance, permselectivity) (*9*) and by the fact that the electrical cell resistance is mainly determined by the electrical resistance of the river water compartment (*1*) (eq 3, ($h_R/(\epsilon^2_R\kappa_R)$).

There is no effect for the number of cells on the power density, indicating that the losses due to shortcut currents (which increases with the number of cells) is minimal (*8*).

Effect of the Residence Time on the Energy Efficiency. At low flow rates (long residence times), it is expected that the energy efficiency is maximal because the equilibrium concentrations can be approached and hydrodynamic power losses are minimal. However, at very low flow rates, losses due to co-ion transport and osmosis start to play a significant role (*9*). Therefore, also for maximal net energy efficiency, there exists an optimal flow.

Figure 4 shows the net power density ($P_{d\text{-}net}$) of a small stack and a large stack as a function of the net energy efficiency (Y_{net}). It should be emphasized that all power measurements were done at maximal power density. At these conditions only 50% of the potential power is harvested (*9*). If maximal power is required, Figure 4 is clear: the small stack performs the best. Maximal net power density for the small stack is 0.71 W/m^2, about twice the value of the large stack (0.40 W/m^2). The net energy efficiency is at this point for 12% for the small stack and 18% for the large stack; the part of energy lost in hydrodynamic friction is 13%, respectively, 16%. Higher energy efficiency is possible by applying a lower flow rate. The upper graph of the small cell in Figure 4 illustrates this: If a net energy efficiency is required of 30%, this is possible at the cost of a reduced net power density of 0.35 W/m^2.

Co-Current or Counter-Current Operation. In many processes, like heat exchange and dialysis, the process can be performed in co-current and in counter-current mode. In most cases, counter-current operation is more efficient due to its higher driving force and it should be investigated whether this is also the case for RED.

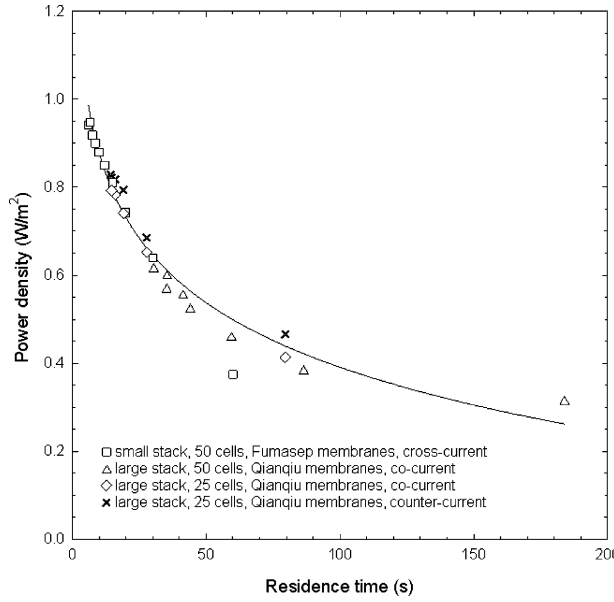

FIGURE 3. Power densities of different stacks and different operational modes. The logarithmic regression line is added to guide the eye.

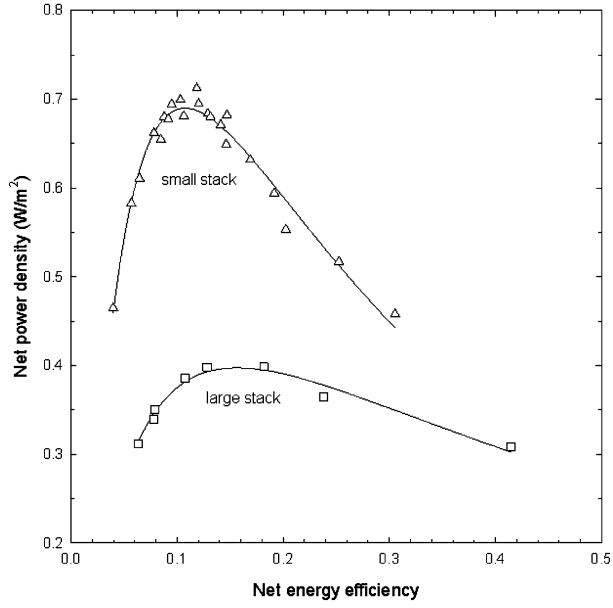

FIGURE 4. Net power density as function of the net energy efficiency in the small and the large stack.

Co-current and counter-current operation were tested in the large stack (Figure 2), equipped with 25 Qianqiu cells. The flow direction was vertical (flow path 25 cm); in the co-current mode, both sea and river water flow upward and in the counter-current mode the direction of the river water flow is inverted. Figure 5 shows the generated power density for both flow directions, it shows that co-current operation yields a little higher power density (about 0.05 W/m^2) compared to counter current flow. This is at first sight rather surprising, because in many processes, counter-current operation is more efficient.

A part of the explanation of this behavior is the existence of two counteracting effects on the generated power density in the cell. In co-current operation the Nernst potential difference (eq 1) is maximal near to the inlet. However, the conductivity of the river water is small at this point (eq 3), resulting in a rather small current. On the outlet side, the Nernst potential difference is lower but the conductivity of

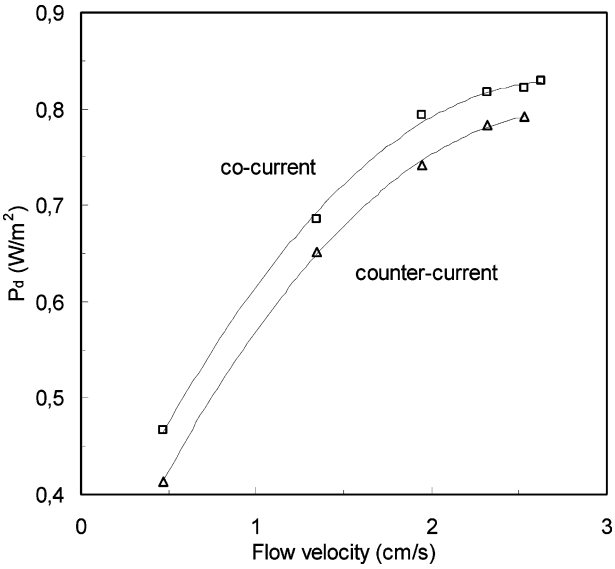

FIGURE 5. Co- and counter-current operation of the large stack.

the river water compartment is higher. This results in a relatively constant power density on each position in the cell. Another part of the explanation is the internal deformation in the stack. In counter-current operation the pressures between sea and river water compartments are very different; only in the middle of the stack, they are equal. Therefore, the spacers in the seawater compartments are compressed on one side of the stack and the river water spacers are compressed at the other side. This may result in local deformations of the flow path with an increase of the hydrodynamic loss.

The higher power densities the co-current mode, has favorable implications on the design of large economical operated RED stacks. By using co-current feed, the pressure between the seawater and the river water compartments is very small. Therefore, leakage around the membranes in the surroundings of the manifolds inside the stack and leakage through pinholes in the membranes is minimal. Besides this, very thin and delicate low electrical resistance membranes can be used with the opportunity to give high power densities. For spacer materials the advantage is that they can be made with a delicate open structure, as necessary for low hydrodynamic losses, and are not compressed due to high pressures differences.

Segmentation of the Electrodes. During the passage of the feedwater through a RED stack, the salt concentration in the river water increases strongly whereas the relative decrease of the salt concentration in the seawater compartment is low. The consequence is that the electrical stack resistance on the inlet side of the river water is higher than on the outlet side (eq 3). Because the ratio of the concentrations is the largest at the inlet side of the river water, the electromotive force (EMF) is maximal on this side. In order to generate maximal power density, the external load should be adjusted to the electrical stack resistance (eq 2). It is evident that the value of the external resistance is a compromise and it is worth investigating whether it is possible to extract more power by means of dividing the electrode into a number of smaller electrodes, each with its own electrical load.

The results are listed in Table 1. The power of an unsegmented stack is 8.23 W, whereas the power of the three segments of a system with divided electrodes is 4.30, 2.49, and 2.31 W, a total of 9.10 W or 11% more then in the unsegmented system.

Because the stack was operated in horizontal direction with a long flow path and consequently high hydrodynamic losses, only relative low flow rates were possible. This implies

TABLE 1. Segmentation of Electrodes

	undivided parallel	divided in three segments		
		segment 1	segment 2	segment 3
open circuit voltage (V)	4.88	5.35	3.89	3.50
terminal voltage (V)	2.40	2.68	1.88	1.74
electrical current (A)	3.42	1.60	1.33	1.33
generated power (W)	8.23	4.30	2.49	2.31
internal resistance (Ω)	0.71	1.67	1.47	1.32

relatively large concentration gradients along the flow paths in the stack. It is plausible that at higher flow rates—with more similar concentrations in the three parts—the effect of segmentation is less. Because segmentation requires additional complicated electronics, it may be questioned whether the small theoretical advantage also holds in practice.

Hydrodynamics; Effect of Flow Path Length. Hydrodynamic losses in the stack are important in the design of a RED generator. We measured the pressure drop due to the fluid resistance in (i) the manifolds, (ii) the bores through the stack, (iii) the spacer filled part of the compartments just around the supply and drain holes and (iv) the part of the spacer filled compartment where a rather uniform flow exists. Fluid resistance of the external tubing is negligible, because this system is well over dimensioned. Likewise, the fluid resistance in the internal bore-holes is very low because these channels are only 3 cm deep. However, the resistance around the inlet and outlet holes in the spacer can be very high. All feedwater enters the compartments radially from these holes with relative high fluid velocities (*13*). We shall refer to this part as "radial spacer resistance". After passing some distance in the spacer filled compartment, the flow is reasonable uniform and we will call this "uniform spacer resistance".

The large stack enables to distinguish between radial and uniform spacer resistance if vertical flow is compared with horizontal flow. The flow path in vertical direction is 25 cm and in horizontal direction 75 cm. However, the distance between the inlets (and also between the outlets) is the same in both directions.

Figure 6 shows pressure as function of the flow rate in the large stack for horizontal (□) and vertical (Δ) operation (both in co-current mode). Data are obtained from different experiments. The slope of the regression line for horizontal operation is almost the same as the slope for vertical operation. This is remarkable because at horizontal operation the length of the flow path is three times the length of the vertical operation. If the uniform spacer resistance contributes only to the total hydrodynamic resistance, a factor 3 should be expected between these slopes.

As stated, a high fluid resistance is expected around the feed holes in the spacer material. Because the inlets (and outlets) are equidistant and the pressure drop is almost the same in both directions, the conclusion is that the main hydrodynamic resistance is caused by these parts. Studies of Dirkse et al. (*13*) support this idea: pictures from modeled velocity fields show high velocities around the inlets and outlets.

There are some possible measures to decrease the fluid resistance. The total cross-sectional area of the supply and drain channels through the stack should not be increased, because in that case the effect of shortcut currents would be unacceptable (*8*). However, it is possible to make more inlet and outlet places with the same total cross-sectional area.

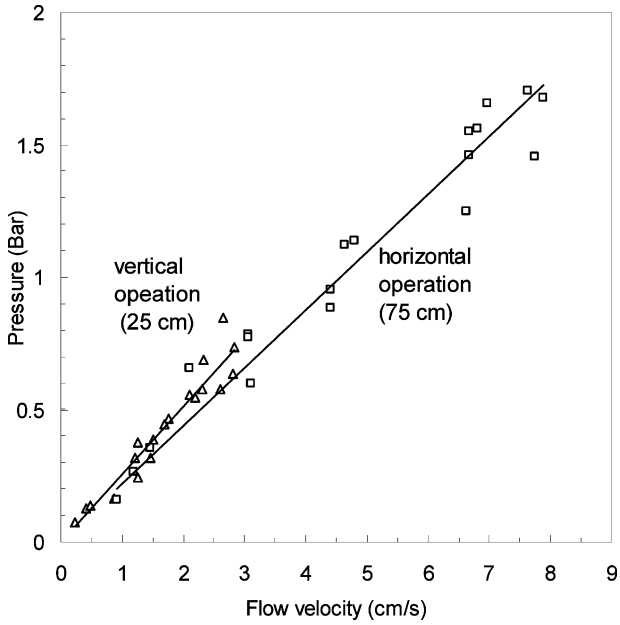

FIGURE 6. Pressure drop as function of the flow velocity in the large stack. Data obtained from different experiments.

Another option is to use special very open spacers around the inlet and outlet holes.

Future Perspectives and Outlook. This study shows that a RED design should cope with the counteracting electrical and hydrodynamic requirements of spacers. With very open spacers, it would be possible to combine a low (perpendicular) electrical cell resistance with a low (lateral) hydrodynamic resistance. Co-current operation enables the use of sophisticated spacers and very thin membranes because the pressure differences between the compartment are low in this case. Net power density and net energy efficiency act also competitive; however, they can be controlled by the flow rate.

Acknowledgments

This work was performed in the TTIW-cooperation framework of Wetsus, centre of excellence for sustainable water technology (www.wetsus.nl). Wetsus is funded by the Dutch Ministry of Economic Affairs, the European Union Regional Development Fund, the province of Fryslân, the city of Leeuwarden and the EZ/Kompas program of the "Samenwerkingsverband Noord-Nederland". The first author thanks the Noordelijke Hogeschool Leeuwarden who facilitated this research by detaching him to Wetsus and the participants of the theme "Energy" theme for their fruitful discussions and their financial support. We thank the Redstack company for financing the large stack, Jan Valk for the making the CAD-CAM drawings of the large stack, Feiko Reinalda, Reinald de Jong, Jan Jansen and Tiara Stoker for their help with the experiments and Bertus Nobach for making Figure 2.

Literature Cited

(1) Veerman, J.; Saakes, M.; Metz, S. J.; Harmsen, G. J. Reverse electrodialysis: performance of a stack with 50 cells on the mixing of sea and river water. *J. Membr. Sci.* **2009**, *327*, 136–144.
(2) Wick, G. L.; Schmitt, W. R. Prospects for renewable energy from sea. *Mar. Technol. Soc. J.* **1977**, *11*, 16–21.
(3) Post, J. W.; Veerman, J.; Hamelers, H. V. M.; Euverink, G. J. W.; Metz, S. J.; Nymeijer, K.; Buisman, C. J. N. Salinity-gradient power: Evaluation of pressure-retarded osmosis and reverse electrodialysis. *J. Membr. Sci.* **2007**, *288*, 218–230.
(4) Pattle, R. E. Production of electric power by mixing fresh and salt water in the hydroelectric pile. *Nature* **1954**, *174* (4431), 660–660.
(5) Pattle, R. E. Electricity from fresh and salt water - without fuel. *Chem. Proc. Eng.* **1955**, *35*, 351–354.
(6) Nijmeijer, K.; Metz, S. J. Salinity Gradient Energy, Chapter 5 from *Sustainability Science and Engineering Vol. 2 Sustainable Water for the Future: Water Recycling versus Desalination* (Eds. Escobar, I. C. and Schäfer, A. I.). .
(7) Post, J. W.; Hamelers, H. V. M.; Buisman, C. J. N. Influence of multivalent ions on power production from mixing salt and fresh water with a reverse electrodialysis system. *J. Membr. Sci.* **2009**, *330*, 65–72.
(8) Veerman, J.; Post, J. W.; Metz, S. J.; Saakes, M.; Harmsen, G. J. Reducing power losses caused by ionic shortcut currents in reverse electrodialysis stacks by a validated model. *J. Membr. Sci.* **2008**, *310*, 418–430.
(9) Veerman, J.; De Jong, R. M.; Saakes, M.; Metz, S. J.; Harmsen, G. J. Reverse electrodialysis: comparison of six commercial membrane pairs on the thermodynamic exergy efficiency and power density. *J. Membr. Sci.* **2009**, *343*, 7–15.
(10) Veerman, J.; Saakes, M.; Metz, S. J.; Harmsen, G. J. Reverse electrodialysis: evaluation of suitable electrode systems. *J. Appl. Electrochem.* **2010**, *40*, 1461–1474.
(11) Forgacs, C. *Generation of electricity by reverse electrodialysis. BGUN-RDA* - 178−78 Ben-Gurion University, Israel, 1978.
(12) Forgacs, C.; O'Brien, R. N. Utilization of membrane processes in the development of non-conventional renewable energy sources. *Chem. Can.* **1979**, *31*, 19–21.
(13) Dirkse, M. H.; Van Loon, W. P. K.; Stigter, J. D.; Post, J. W.; Veerman, J.; Bot, G. P. A. Extending potential flow modelling of flat-sheet geometries as applied in membrane-based systems. *J. Membr. Sci.* **2008**, *325*, 537–545.
(14) Post, J. W.; Hamelers, H. V. M.; Buisman, C. J. N. Energy recovery from controlled mixing salt and fresh water with a reverse electrodialysis system. *Environ. Sci. Technol.* **2008**, *42*, 5785–5790.

ES1009345